Vol. 508: 201–209, 2014
doi: 10.3354/meps10813

MARINE ECOLOGY PROGRESS SERIES
Mar Ecol Prog Ser

Published August 4

Density of reef sharks estimated by applying an agent-based model to video surveys

Mathew A. Vanderklift[1,*], Fabio Boschetti[1], Clovis Roubertie[1], Richard D. Pillans[2], Michael D. E. Haywood[2], Russell C. Babcock[2]

[1]CSIRO Wealth from Oceans Flagship, Private Bag 5, Wembley, Western Australia 6913, Australia
[2]CSIRO Wealth from Oceans Flagship, 41 Boggo Rd, Dutton Park, Queensland 4102, Australia

ABSTRACT: Policies on harvesting and conservation are developed in response to information about trends in the abundance of species, so making accurate estimates of abundance is important. However, estimating the abundance of sparsely distributed species is challenging, especially where direct observations are difficult. We collected observations of blacktip reef sharks *Carcharhinus melanopterus* by using remote underwater video cameras, and developed an agent-based model to generate estimates of the density of sharks from the frequency of observations made using the video. We augmented these observations with diel patterns in detections in different habitats of *C. melanopterus* with surgically implanted acoustic transmitters. Median estimates of density ranged from 2–9 ind. km^{-2} at noon to 20–90 ind. km^{-2} at dusk, depending on whether modelled movement paths were random or directional. These estimates suggest that individuals might exhibit diel patterns in movement, with directional movement to the reef flat during dusk. Data from tagged individuals supported this hypothesis, with more detections recorded from reef flat habitat during early evening and early morning than at other times of day. Estimates of density were among the highest reported for *C. melanopterus*. The agent-based model approach is flexible, and can be extended to simulate a range of behaviours and other types of observations.

KEY WORDS: Camera trap · *Carcharhinus melanopterus* · Lévy flight · Ningaloo · Random walk · Rarity

INTRODUCTION

Large predators can play a key role in determining the abundance and composition of their prey (Ray et al. 2005, Estes et al. 2011). As a consequence, declines in the abundance of these predators sometimes result in changes in the abundance of prey, and these can further cascade down to lower trophic levels (Hairston et al. 1960, Prugh et al. 2009). Because of their integral role in ecosystems, it is important to get accurate estimates of the abundances of large predators — a task which can be challenging because these species are often rare, sparsely distributed, or elusive, characteristics that make estimating abundance particularly difficult (Thompson 2004). Camera traps are frequently used to estimate the abundance of species with these characteristics (O'Connell et al. 2011). They have been used to generate estimates of the density of individuals and the number of species, and can also be used to generate insights about behaviour or demographic parameters (Head et al. 2013).

The methods that are most typically used to quantify the abundances of coastal sharks are visual censuses by divers, observations using video cameras (usually employing the use of bait as an attractant) and mark-recapture methods based on tagging. Each of these methods has its own set of biases and uncertainties, and different methods can yield very different estimates of abundance (McCauley et al. 2012).

*Corresponding author: mat.vanderklift@csiro.au

For example, visual censuses can introduce biases associated with behavioural responses to the presence of divers, and uncertainties associated with non-instantaneous counts (Ward-Paige et al. 2010), while the use of bait might yield results that vary according to the dispersal of olfactory compounds and interspecies interactions around the bait (Bassett & Montgomery 2011, Trenkel & Lorance 2011).

Because policies about harvesting or conserving sharks are influenced by advice determined — at least partly — from the results of such surveys (Techera & Klein 2011), it is important to understand the uncertainties associated with different methods, and also to attempt to use methods that best reflect the true density of sharks (i.e. the number of individual sharks per unit area). Observations made using remote underwater video cameras without bait offer perhaps the best opportunity to attain this goal, because they avoid the biases that are associated with divers and bait; the cameras themselves might introduce some biases (e.g. the potential to attract or deter sharks), but any biases are likely to be minor compared to those associated with divers and bait.

However, observations made using video cameras have one critical constraint — they do not provide estimates of density. Rather, they provide information about the frequency of observation or, in some cases, relative abundance. In situations in which individuals can be distinguished, capture-recapture models can be used (Marshall & Pierce 2012), but in situations in which individuals cannot be distinguished, or in which recapture rates are very low, these models are less useful. Here, we report the results of a study using an agent-based model that incorporates information about shark behaviour to provide estimates of density derived from video observations. We use this method to estimate the density of the blacktip reef shark *Carcharhinus melanopterus* (Quoy & Gaimard, 1824) found in reef flat habitat on Ningaloo Reef (Australia) at 2 times of day: solar noon and just before sunset (dusk). The general approach we used involves: (1) an agent-based model of the movement tracks of individual sharks, (2) the use of this model to estimate the frequency that sharks would be detected by video cameras (with associated uncertainty) and (3) a comparison between the modelled frequency of observation and the actual frequencies of shark observations yielded by video camera deployments.

Estimating shark abundance in this manner is an inverse problem, that is, a problem in which solutions are generated by generating estimates of parameters from observations (Tarantola 1987, Symons & Boschetti 2012). Because of this, a different approach is needed to that used to solve forward problems, those in which calculations are made based on some parameters (e.g. the density of sharks) in order to reproduce some observations (e.g. the frequency of observations of sharks from video camera deployments).

If the movement tracks of individual sharks could be described by simple statistics, allowing estimation of the probability of an observation of a shark at a given location, then the inverse problem described above would be fairly simple. This would occur if, for example, the movement of each individual was unconstrained, such as might occur if an individual were foraging for a uniformly or randomly distributed resource in an essentially boundless area. This is roughly the idea on which most algorithms to establish animal abundance are based. However, when the movement of individuals is constrained, for example by coastline, reefs, heterogeneous habitat, interference with other individuals, or ocean currents, the probability of observing a shark at a specific location can no longer be described by a simple formula, but needs to be computed. This is what our agent-based model does.

MATERIALS AND METHODS

Study area and video camera deployments

We surveyed 16 sites in and around the Mandu Sanctuary Zone (1185 ha) in the Ningaloo Marine Park (22° 04′ S, 113° 53′ E): 8 sites were in the Sanctuary Zone (SZ) and 8 sites were in the adjoining Recreation Zone (RZ). We focused the surveys on reef flat habitat, which is typically shallow (<3 m) and dominated by tabulate coral of the genus *Acropora*. Surveys were conducted between 1 and 6 June 2010. We surveyed each site at 2 times of day — solar noon and dusk. At each site, we deployed a single video camera (Sony DCR-HC15E) in a housing mounted on a concrete block. Cameras recorded from at least 60 min before sunset and for at least 60 min following solar noon; recording times ranged from 60 to 94 min (mean ± SD: 87 ± 7 min).

In the laboratory, video footage was viewed on a computer screen, and all sharks passing through the field of view were recorded. We recorded the time and duration (in seconds) of each observation. From these recordings, we calculated the observed frequency of shark detection, F_{obs} as the ratio between the total time all sharks were observed in front of a camera, t_{sh}, and the total filming time, t_c.

The video camera deployments yielded 1611 min of video at noon (average: 89 min) and 1258 min at dusk (average: 84 min). Three species of sharks were observed (Table 1). Sharks were observed at 15 sites (94%) at dusk and 4 sites (25%) at noon. The most frequently observed species was *Carcharhinus melanopterus*, which was observed at 13 sites (81%) at dusk and 4 sites (25%) at noon. Subsequent modelling therefore focussed on this species.

The agent-based model

In the agent-based model, the movement of individual sharks is constrained by barriers and influenced by habitat. We extracted the coastline and reef crest (both barriers to movement) from Google Earth. We represented these features, and the reef flat, in a model domain encompassing 3400 × 5050 m, with grid cells of 3 m × 3 m (Fig. 1). The model requires 3 main components: (1) statistical distributions describing the lengths of straight-line movements and the turning angles, (2) an algorithm controlling the way each individual interacts with habitats and with obstacles to movement and (3) a way to determine when each modelled individual can be 'detected' by the cameras in the model.

In the current implementation we did not account for how sharks interact with each other or how they interact with the video camera. However, should these behaviours be deemed important, and should information about them become available, they could be included in the model.

Shark movement patterns

In our model the position of a shark at time step i is given as:

$$x_i = x_{i-1} + r_i \cos\alpha_i;\ \ y_i = y_{i-1} + r_i \sin\alpha_i \qquad (1)$$

where x and y determine the position of the shark (in Cartesian coordinates), r is the length of a straight-line movement performed by the shark (hereafter referred to as a step) and α is the orientation of the step. The variables r and α were chosen stochastically from the following distributions:

$$P(r) \sim r^{-\mu} \text{ for } r \in [minstep, maxstep] \qquad (2)$$

and

$$\alpha_i = \alpha_{i-1} + \theta_i$$
$$\theta_i = (1 - k_{dir})\,\varepsilon_i + k_{dir}\,\tau_i,\ k_{dir} \in [0,1] \qquad (3)$$

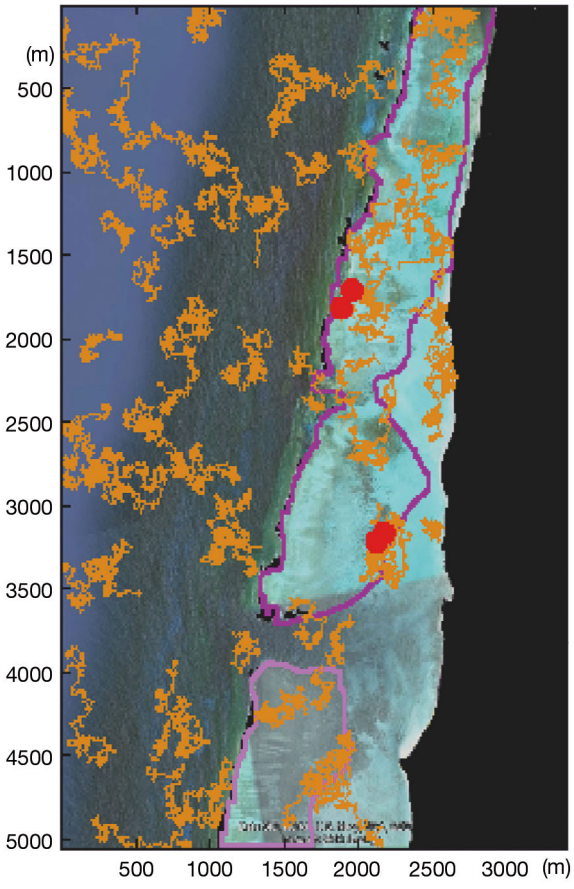

Fig. 1. An example of the movement patterns reproduced by the model, showing 40 movement tracks (orange lines), for $k_{dir} = 0$ (where k_{dir} is the form of the path an individual travels and 0 = fully random), plotted over the study area. Magenta boundaries show the reef flat habitat. Black represents land and reef crest (barriers to movement). Red dots indicate where cameras were located in field surveys

Table 1. Summary of species of sharks observed, number of sites at which each species was recorded, the average duration (Avg. dur.) each individual spent in the field of view (in seconds, calculated only for sites at which the species was observed), and the frequency of shark detection (F_{obs}) for *Carcharhinus melanopterus*

Species	Noon			Dusk		
	No. of sites	Avg. dur. (s)	F_{obs}	No. of sites	Avg. dur. (s)	F_{obs}
Carcharhinus melanopterus	4	12	0.0006	13	21	0.0056
Negaprion acutidens	0	–		2	15	
Triaenodon obesus	1	7		4	5	

In Eq. (2), P(r) is the probability of occurrence of a step of length r, *minstep* and *maxstep* are the minimum and maximum step lengths, respectively (Sims et al. 2008, Humphries et al. 2010), and μ is the scaling exponent, which determines how step lengths are distributed within this range (in particular the relative distribution of small versus large steps, which determines the complexity of the path moved by each individual, as well as the total area covered in a given time interval). Ideally, μ, *minstep* and *maxstep* should be determined empirically from observations of shark movement, but such information was not available, so we chose to use *minstep* = 3 m, *maxstep* = 100 m, and 3 values for μ to encompass the expected range (1.7, 2 and 2.3). These values were chosen based on theoretical and empirical studies of a range of taxa, including carcharhinid sharks (Sims et al. 2008, 2012, Humphries et al. 2010). We chose a lower *maxstep* than that observed in many of the species in those studies, because there is some evidence that the step lengths exhibited by *C. melanopterus* are shorter than those of other sharks (Papastamatiou et al. 2009).

Depending on the value of the exponent μ, Eq. (2) reproduces 2 behavioural patterns commonly described in the literature: Lévy flight ($1 < \mu \leq 3$) and Brownian motion ($\mu > 3$). Empirical observations suggest that Lévy flights are suitable for modelling foraging behaviour in animals (Viswanathan et al. 1996, Marell et al. 2002, Reynolds et al. 2007a,b), including sharks (Sims et al. 2008, 2012, Humphries et al. 2010). With $\mu \approx 2$, Lévy flight should provide an optimal search pattern (Sims et al. 2008, 2012, Viswanathan et al. 2008, Humphries et al. 2010, James et al. 2011, Reynolds 2012), and, consequently, it is often assumed to be a biologically justified model for foraging animals. However, the choice is not critical to our approach, and a different distribution could be adopted by modifying the algorithm.

In Eq. (3), θ is the turning angle, defining the change of direction between 2 consecutive steps. Here ε_i is drawn from a uniform random distribution, and τ_i is the direction towards a desired location, in the case of oriented movement. For our discussion, the crucial parameter in this equation is $k_{dir} \in [0,1]$ (where k_{dir} is the form of the path an individual travels) which determines a balance between fully random ($k_{dir} = 0$) and directional ($k_{dir} = 1$) movement. The relationship $0.05 < k_{dir} < 0.3$ has been suggested to provide a realistic description of animal movement (Nams 2006). Eq. (2) allows each individual to follow paths which are constrained by the distributions in Eq. (3). However, movement is further constrained by the coastline and model boundaries. The coastline and model boundaries are treated as 'hard' boundaries which an individual cannot cross and which require movement away. The rationale for treating the model boundary in this way lies in the fairly short simulation time (90 min), which led us to treat both the shark population and the study area as closed. Similarly, the reef crest is treated as a boundary that a shark cannot cross. We included 2 broad 'habitats', the reef flat habitat in which the video cameras were deployed and the rest of the coastal waters (see Fig. 1). We ran the model with $k_{dir} = 0$, simulating unoriented Lévy flight (Viswanathan et al. 1999, Bartumeus et al. 2002, Sims et al. 2008, Humphries et al. 2010, James et al. 2011) and with $k_{dir} = 0.25$, which, together with τ_i, yields directional movement towards the reef flat habitat (Nams 2006).

In our model sharks move at a constant speed. The most appropriate average swimming speed is uncertain, so we used 3 values (0.5, 0.7 and 1 m s^{-1}) based on literature values: swimming speeds for *C. melanopterus* and other species of carcharhinid sharks encompass this range (Webb & Keyes 1982, Sundström et al. 2001, McCauley et al. 2012).

In the final step, we included cameras in the model and defined the area within which they could record an observation (our video cameras were set to the widest angle and were fitted with an additional wide-angle lens so the angle of view was approximately 45°; based on field measurements, we determined that the maximum distance from the camera at which an individual's species could reliably be identified was 6 m) and recorded the duration each individual spent within the area in which they could be observed. This provided us with F_{mod}, the modelled frequency of a shark being observed:

$$F_{mod} = \frac{t_{sh}}{t_{sim} n_c} \quad (4)$$

where t_{sh} is the time a shark has spent in the cameras' visual field, t_{sim} is the simulation time and n_c is the number of cameras.

Model runs and statistics of shark abundance

Because some parameters governing shark movement (μ, speed, *minstep* and *maxstep*) were derived from estimates for related species, or from theoretical studies, we evaluated the extent to which these parameters affect the result. Simulations suggested that *minstep* and *maxstep* have a minor influence on the results (see the Supplement at www.int-res.com/

articles/suppl/m508p201_supp.pdf), so we decided to fix their values to 3 and 100 m, respectively. To account for the uncertainty in the remaining parameters, we conservatively decided to allow them to vary within ranges.

In addition to parameter uncertainty, simulation results can vary considerably between model runs due to the inherent stochasticity in Lévy flight. In order to account for this, we ran 100 simulations for each parameter combination, resulting in 900 simulations. This gives an estimated distribution of F_{mod}.

F_{mod} is a function of the number of simulated sharks. By calculating F_{mod} for shark populations of different sizes, we obtained F^s_{mod}, where s is the density. F^s_{mod} represents the modelled distribution of shark observations, as a function of the density, which accounts for the uncertainty in our knowledge of shark behaviour as well as its inherent stochasticity.

The last step in our approach involves comparing the observations from field deployments, F_{obs}, to modelled observations, F^s_{mod}, to determine the value of s that provides the best match (Fig. 2). For a given value of x (e.g. 40 sharks km^{-2}), the location at which a line parallel to the y-axis intersects a given percentile (e.g. 80th percentile), gives the F^s_{mod} below which 80 % of observations lies. In other words, a point (x,y) in Fig. 2 shows the percentile of models run with a density x of sharks which gives modelled shark observations $F^s_{mod} < y$.

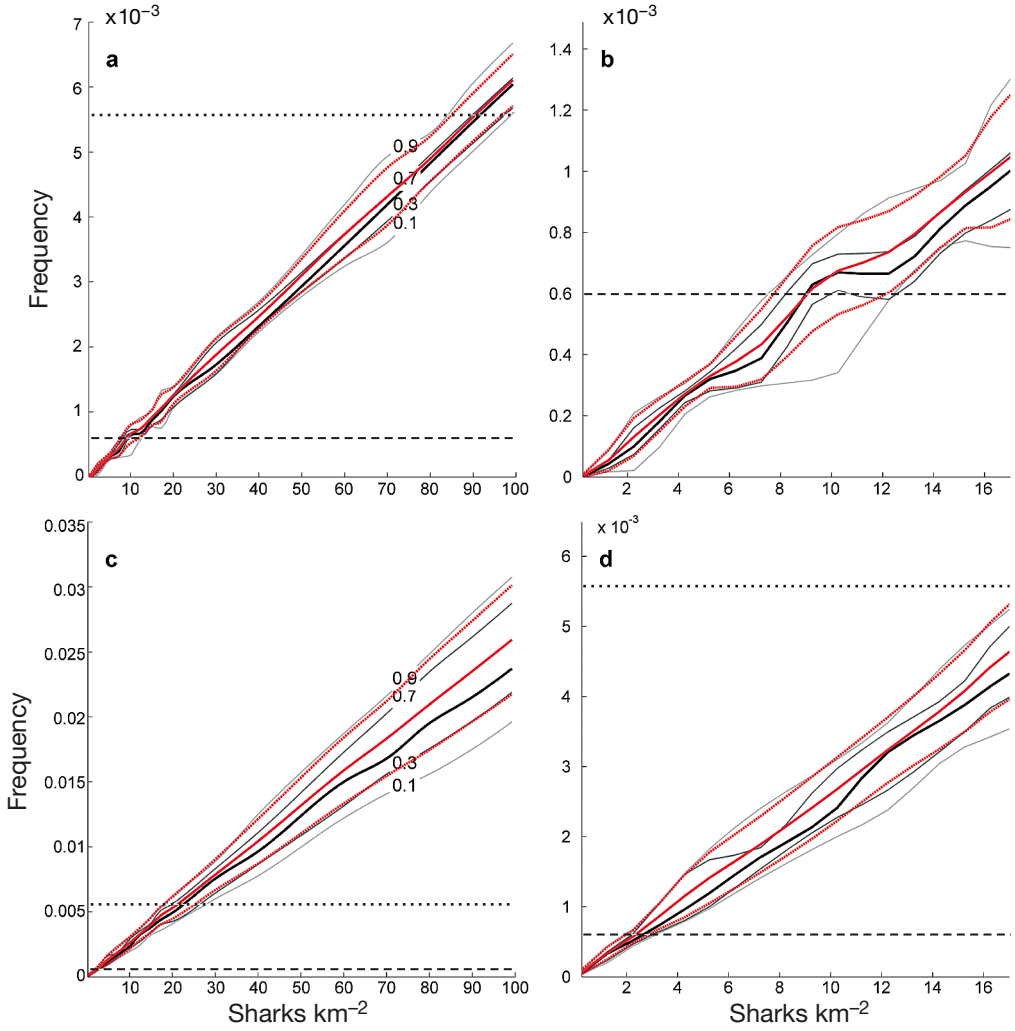

Fig. 2. Modelled frequency of observations (F^s_{mod}) plotted against (modelled) shark density, for (a) k_{dir} = 0 (with lower left part of the plot magnified in Panel b) and for (c) k_{dir} = 0.25 (with lower left part of the plot magnified in Panel d). The x-axis represents density s (ind. km^{-2}); the y-axis represents F^s_{mod}. The distribution of all 900 model runs is represented in terms of percentiles: the thick black line corresponds to the median; thin grey lines correspond to the 10, 30, 70 and 90 percentiles. The solid red line represents the mean of the 900 model runs dotted red lines represent the SD. The horizontal lines indicate the observed frequency of observation (F_{obs}) for dusk (dotted) and noon (dashed)

Acoustic tracking

Because the results of agent-based modelling suggested that the best outcomes were achieved when k_{dir} was varied between noon and dusk and between reef flat and other coastal habitats (see 'Results'), we examined the results of an acoustic tagging study for evidence that this pattern would be supported by the available data. The acoustic tagging study was undertaken in Mangrove Bay (21° 57′ S, 113° 56′ E), approximately 10 km north of our study area. The study has been operating since 2008, and a total of 60 acoustic receivers (VR2; Vemco) have been deployed over an area of approximately 28 km^2. Fifteen individuals of *C. melanopterus* (size range: 78 to 134 cm fork length) have been implanted with coded transmitters (V13 and V16, Vemco; intervals between transmissions averaged between 60 and 80 s), following the procedure outlined in Pillans et al. (2011). We restricted the dataset to 11 individuals for which detections spanned a period of at least 100 d. We then calculated the overall mean number of detections in 60 min intervals to examine diel patterns in detection. This procedure was conducted for 5 distinct habitats: reef flat (6 receivers, 39 683 detections), lagoon (24 receivers, 80 272 detections), reef slope (24 receivers, 32 836 detections), reef pass (2 receivers, 7910 detections) and Mangrove Bay (4 receivers, 8629 detections).

RESULTS

In order to determine the expected density of sharks (ind. km^{-2}) we matched the modelled values of F^s_{mod} that corresponded to F_{obs} (Table 1, Fig. 2). For k_{dir} = 0, the F^s_{mod} median curve (thick black line) suggests a density of approximately 90 ind. km^{-2} at dusk (80% CI: 80–100) and 9 ind. km^{-2} at noon (80% CI: 8–12). For k_{dir} = 0.25, the F^s_{mod} suggests a density of approximately 20 ind. km^{-2} at dusk (80% CI: 16–26) and 2 ind. km^{-2} at noon (80% CI: 1.5–3.0).

It might be reasonable to assume that k_{dir} = 0.25 at dusk (when they were more frequently observed on the reef flat) and k_{dir} = 0 at noon (when sharks were assumed not to be foraging). In this case the 2 estimates of density would be slightly different, with 80% confidence intervals of 16 to 26 ind. km^{-2} at dusk (median = 20) and 8 to 12 ind. km^{-2} at noon (median = 9). This result could be produced if some individuals leave the reef flat during certain times of the day, returning before or during dusk.

Results from acoustic receivers in Mangrove Bay provided some support for this hypothesis; individual *Carcharhinus melanopterus* were detected by receivers in reef flat habitat more frequently in the evening and in the early morning than at other times of day (Fig. 3). This result would be expected if individuals were undertaking oriented movements to the reef flat at these times of day, so that k_{dir} = 0.25 might be appropriate. Diel patterns in detection were generally not clear for the other habitats included in acoustic tracking, although there was also a pattern of higher detection rates on the reef slope during daylight hours.

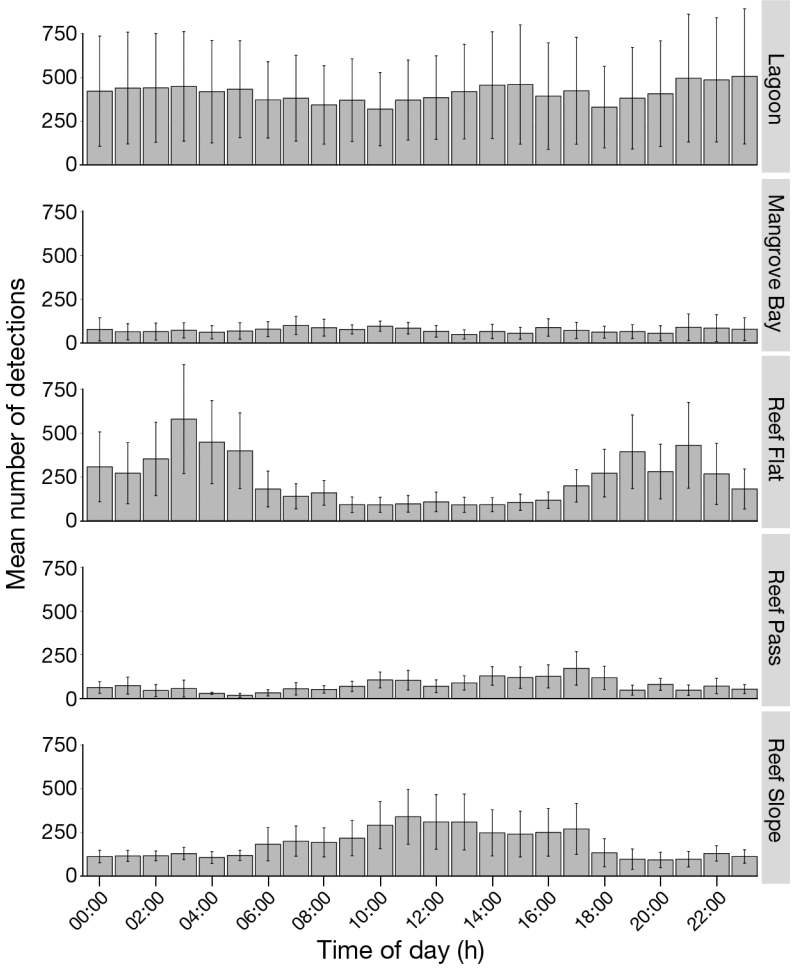

Fig. 3. Mean number of detections (±SE) of *Carcharhinus melanopterus* with surgically implanted acoustic tags, recorded by receivers in 5 different habitats at different times of day (binned into 60 min categories)

DISCUSSION

The blacktip reef shark *Carcharhinus melanopterus* was the most frequently observed species of shark in the reef flat habitat, where we conducted our surveys. Our model-based method for estimating the density of *C. melanopterus* yielded (median) estimates of 2 to 9 ind. km^{-2} at solar noon and 20 to 90 ind. km^{-2} at dusk. These estimates are at the upper range of estimates reported by other authors (Table 2). For example, of 45 underwater visual census (UVC) surveys around islands in the Pacific Ocean, only 4 islands yielded estimates of >10 ind. km^{-2} (Nadon et al. 2012); the highest of these was at Palmyra, where the estimate was 91 ind. km^{-2}. High densities have also been reported at Aldabra (62 ind. km^{-2}), from mark and recapture surveys (Stevens 1984). In contrast, surveys of 8 reefs on the Great Barrier Reef yielded very low estimates of *C. melanopterus* density (1 individual recorded during surveys of 8 reefs; Ayling & Choat 2008). Direct comparisons among these estimates are complicated by the different methods used: different methods can yield different estimates of density (McCauley et al. 2012), and UVC methods can yield over-estimates of density (Ward-Paige et al. 2010). In addition, many of the surveys focussed on forereef habitats, where *C. melanopterus* often occurs in low density and other species of sharks are more abundant (Ayling & Choat 2008, Nadon et al. 2012) — this pattern is also observed at Ningaloo Reef (M. A. Vanderklift, M. D. E. Haywood & R. C. Babcock unpubl. data).

Our surveys yielded a higher frequency of observations at dusk than at solar noon. This pattern could be generated by 2 (non-exclusive) mechanisms: *C. melanopterus* might exhibit diel patterns in habitat use or in movement patterns (for example swimming speed). Both hypotheses could be supported by the results yielded by detection patterns of individuals with surgically implanted acoustic transmitters. We also note that the median estimates of density at dusk with oriented movement — which would be applicable if individuals were moving towards this habitat (20 ind. km^{-2}) — were slightly higher than those obtained for noon with unoriented movement, which would be applicable if individuals were not exhibiting diel patterns in habitat use (9 ind. km^{-2}).

This pattern is also congruent with observations of the activity patterns of *C. melanopterus* and other species of sharks; some studies using acoustic tags have found diel patterns in detection that imply changes in habitat use (Papastamatiou et al. 2010, Speed et al. 2011). However, data on diel patterns of density in different habitats are few. In one study, McCauley et al. (2012) found no difference in the density of sharks between day and evening. Movement patterns may also be associated with tides. *C. melanopterus* has been observed to move into shallow habitats during rising tides (Stevens 1984), but this does not account for our observations, as the dusk surveys were conducted on a falling tide, while solar noon coincided with a rising tide.

In our model the main variables are given by μ, *minstep*, *maxstep*, k_{dir} and swimming speed, each of which can be altered as appropriate for different species. However, our approach does not rely on a specific model of animal behaviour, because the framework has the flexibility to accommodate different types of behaviour. An exponential distribution of step sizes, Brownian motion, or other movement patterns could be implemented and included in the approach as appropriate.

Additional steps to implement the model in other situations include: definition of the spatial elements of the model domain (i.e. the dimensions of the area, the grid size, obstacles to movement) and how individuals behave (e.g. whether they interact with each other, with the video cameras, or with map borders;

Table 2. Densities of *Carcharhinus melanopterus* yielded by this study and others. UVC: underwater visual census

Density (ind. km^{-2})	Method	Location	Study
9	Noon, k_{dir} = 0	Ningaloo Reef	This study
90	Dusk, k_{dir} = 0	Ningaloo Reef	This study
2	Noon, k_{dir} = 0.25	Ningaloo Reef	This study
20	Dusk, k_{dir} = 0.25	Ningaloo Reef	This study
0	UVC	Main Hawaiian Islands	Nadon et al. (2012)
0	UVC	Northwest Hawaiian Islands	Nadon et al. (2012)
0–2.7	UVC	Great Barrier Reef	Ayling & Choat (2008)
0.6–8.7	UVC	American Samoa	Nadon et al. (2012)
0–14.3	UVC	Mariana Islands	Nadon et al. (2012)
62	Mark-recapture	Aldabra Island	Stevens (1984)
0–91.2	UVC	Pacific Remote Islands	Nadon et al. (2012)

whether they retain a memory of a previous path). Implementation involves decisions about the range of values associated with each parameter, such as we did for swimming speed and μ. In addition, because of the stochasticity of the model, a decision is needed about how many times to repeat each run (in our case, we chose 100 times for each combination of parameters).

Compared to traditional approaches to determine animal abundance (e.g. linear models based on data collected from visual censuses or capture-recapture models), the proposed method is time-consuming to implement and to run. However, methods for estimating abundance should ideally account for patterns of animal movement and interactions with the environment. Methods which do not require the user to make decisions on these processes will inevitably make the decision for the user, in ways which are often hidden behind the maths. In such cases the user might not know how results depend on those implicit choices. The strength of the agent-based model is the flexibility it provides, as well as the explicit incorporation of decisions about parameters. In addition, no assumptions are made about the distribution of individuals; for example, they can be distributed uniformly, randomly, or according to any other pattern. However, if the modelled distribution F^s_{mod} departs substantially from a uniform distribution, effort should be allocated towards choosing a suitable statistic for comparisons with F_{obs}.

The agent-based model enabled us to generate estimates of density for blacktip reef sharks from remote underwater video observations that provided data on detection frequency. The estimates yielded by this method are among the highest reported for this species. Studies of sparsely distributed or elusive species can be improved by combining methods — for example studies that have integrated data from DNA-based or telemetry studies with data from camera trap surveys have yielded estimates that are more precise than those obtained with camera traps alone (Gopalaswamy et al. 2012, Sollmann et al. 2013). Because of the ecological importance of sharks, and the benefit that accurate estimates can provide in the development of policies concerning harvesting and conservation, continued refinement of the methods is necessary.

Acknowledgements. We thank D. Thomson, K. Cook, C. Seytre and J.-B. Cazes for assistance in the field and laboratory. This research was supported by the CSIRO Wealth from Oceans Flagship and the Western Australian Department of Environment and Conservation.

LITERATURE CITED

Ayling AM, Choat JH (2008) Abundance patterns of reef sharks and predatory fishes on differently zoned reefs in the offshore Townsville region: final report to the Great Barrier Reef Marine Park Authority. Great Barrier Reef Marine Park Authority, Townsville

Bartumeus F, Catalan J, Fulco U, Lyra M, Viswanathan G (2002) Optimizing the encounter rate in biological interactions: Lévy versus Brownian strategies. Phys Rev Lett 88:097901

Bassett DK, Montgomery JC (2011) Investigating nocturnal fish populations *in situ* using baited underwater video: with special reference to their olfactory capabilities. J Exp Mar Biol Ecol 409:194–199

Estes JA, Terborgh J, Brashares JS, Power ME and others (2011) Trophic downgrading of planet earth. Science 333:301–306

Gopalaswamy AM, Royle JA, Delampady M, Nichols JD, Karanth KU, Macdonald DW (2012) Density estimation in tiger populations: combining information for strong inference. Ecology 93:1741–1751

Hairston NG Jr, Smith FE, Slobodkin LB (1960) Community structure, population control, and competition. Am Nat 94:421–425

Head JS, Boesch C, Robbins MM, Rabanal LI, Makaga L, Kühl HS (2013) Effective sociodemographic population assessment of elusive species in ecology and conservation management. Ecol Evol 3:2903–2916

Humphries NE, Queiroz N, Dyer JRM, Pade NG and others (2010) Environmental context explains Lévy and Brownian movement patterns of marine predators. Nature 465: 1066–1069

James A, Plank MJ, Edwards AM (2011) Assessing Lévy walks as models of animal foraging. J R Soc Interface 8: 1233–1247

Marell A, Ball JP, Hofgaard A (2002) Foraging and movement paths of female reindeer: insights from fractal analysis, correlated random walks, and Levy flights. Can J Zool 80:854–865

Marshall AD, Pierce SJ (2012) The use and abuse of photographic identification in sharks and rays. J Fish Biol 80: 1361–1379

McCauley DJ, McLean KA, Bauer J, Young HS, Micheli F (2012) Evaluating the performance of methods for estimating the abundance of rapidly declining coastal shark populations. Ecol Appl 22:385–392

Nadon MO, Baum JK, Williams ID, McPerson JM and others (2012) Re-creating missing population baselines for Pacific reef sharks. Conserv Biol 26:493–503

Nams VO (2006) Detecting oriented movement of animals. Anim Behav 72:1197–1203

O'Connell AF, Nichols JD, Karanth KU (2011) Camera traps in animal ecology. Springer, Dordrecht

Papastamatiou YP, Lowe CG, Caselle JE, Friedlander AM (2009) Scale-dependent effects of habitat on movements and path structure of reef sharks at a predator-dominated atoll. Ecology 90:996–1008

Papastamatiou YP, Friedlander AM, Caselle JE, Lowe CG (2010) Long-term movement patterns and trophic ecology of blacktip reef sharks (*Carcharhinus melanopterus*) at Palmyra Atoll. J Exp Mar Biol Ecol 386:94–102

Pillans R, Babcock R, Patterson T, How J, Hyndes G (2011) Adequacy of zoning in the Ningaloo Marine Park: final report. CSIRO Marine & Atmospheric Research,

Brisbane
Prugh LR, Stoner CJ, Epps CW, Bean WT, Ripple WJ, Laliberte AS, Brashares JS (2009) The rise of the mesopredator. Bioscience 59:779–791
Ray JC, Redford KH, Steneck RS, Berger J (2005) Large carnivores and the conservation of biodiversity. Island Press, Washington, DC
Reynolds AM (2012) Truncated Lévy walks are expected beyond the scale of data collection when correlated random walks embody observed movement patterns. J R Soc Interface 9:528–534
Reynolds AM, Smith AD, Menzel R, Greggers U, Reynolds DR, Riley JR (2007a) Displaced honey bees perform optimal scale-free search flights. Ecology 88:1955–1961
Reynolds AM, Smith AD, Reynolds DR, Carreck NL, Osborne JL (2007b) Honeybees perform optimal scale-free searching flights when attempting to locate a food source. J Exp Biol 210:3763–3770
Sims DW, Southall EJ, Humphries NE, Hays GC and others (2008) Scaling laws of marine predator search behaviour. Nature 451:1098–1102
Sims DW, Humphries NE, Bradford RW, Bruce BD (2012) Lévy flight and Brownian search patterns of a free-ranging predator reflect different prey field characteristics. J Anim Ecol 81:432–442
Sollmann R, Gardner B, Chandler RB, Shindle DB, Onorato DP, Royle JA, O'Connell AF (2013) Using multiple data sources provides density estimates for endangered Florida panthers. J Appl Ecol 50:961–968
Speed CW, Meekan MG, Field IC, McMahon CR and others (2011) Spatial and temporal movement patterns of a multi-species coastal reef shark aggregation. Mar Ecol Prog Ser 429:261–275
Stevens JD (1984) Life-history and ecology of sharks at Aldabra Atoll, Indian Ocean. Proc R Soc Lond B Biol Sci 222:79–106
Sundström LF, Gruber SH, Clermont SM, Correia JPS and others (2001) Review of elasmobranch behavioral studies using ultrasonic telemetry with special reference to the lemon shark, *Negaprion brevirostris*, around Bimini Islands, Bahamas. Environ Biol Fishes 60:225–250
Symons J, Boschetti F (2012) How computational models predict the behavior of complex systems. Found Sci 18: 809–821
Tarantola A (1987) Inverse problem theory. Elsevier, Amsterdam
Techera EJ, Klein N (2011) Fragmented governance: reconciling legal strategies for shark conservation and management. Mar Policy 35:73–78
Thompson WL (2004) Sampling rare or elusive species: concepts, designs, and techniques for estimating population parameters. Island Press, Washington, DC
Trenkel VM, Lorance P (2011) Estimating *Synaphobranchus kaupii* densities: contribution of fish behaviour to differences between bait experiments and visual strip transects. Deep-Sea Res I 58:63–71
Viswanathan GM, Afanasyev V, Buldyrev SV, Murphy EJ, Prince PA, Stanley HE (1996) Levy flight search patterns of wandering albatrosses. Nature 381:413–415
Viswanathan GM, Buldyrev SV, Havlin S, da Luz MG, Raposo EP, Stanley HE (1999) Optimizing the success of random searches. Nature 401:911–914
Viswanathan GM, Raposo EP, da Luz MGE (2008) Lévy flights and superdiffusion in the context of biological encounter and random searches. Phys Life Rev 5: 133–150 doi:10.1016/j.plrev.2008.03.002
Ward-Paige C, Flemming JM, Lotze HK (2010) Overestimating fish counts by non-instantaneous visual censuses: consequences for population and community descriptions. PLoS ONE 5:e11722
Webb PW, Keyes RS (1982) Swimming kinematics of sharks. Fish Bull 80:803–812

Editorial responsibility: Ivan Nagelkerken, Adelaide, South Australia, Australia

Submitted: July 18, 2013; Accepted: April 2, 2014
Proofs received from author(s): June 10, 2014